

General Disclaimer

One or more of the Following Statements may affect this Document

- This document has been reproduced from the best copy furnished by the organizational source. It is being released in the interest of making available as much information as possible.
- This document may contain data, which exceeds the sheet parameters. It was furnished in this condition by the organizational source and is the best copy available.
- This document may contain tone-on-tone or color graphs, charts and/or pictures, which have been reproduced in black and white.
- This document is paginated as submitted by the original source.
- Portions of this document are not fully legible due to the historical nature of some of the material. However, it is the best reproduction available from the original submission.



(NASA-CR-165080) A MODIFIED DODGE ALGORITHM
FOR THE PARABOLIZED NAVIER-STOKES EQUATION
AND COMPRESSIBLE DUCT FLOWS Final Report,
15 Apr. 1978 - 30 Nov. 1981 (Old Dominion
Univ., Norfolk, Va.) 34 p HC A03/MF A01

N82-16363

Unclas
G3/34 07361

DEPARTMENT OF MATHEMATICAL SCIENCES
SCHOOL OF SCIENCES AND HEALTH PROFESSIONS
OLD DOMINION UNIVERSITY
NORFOLK, VIRGINIA

A MODIFIED DODGE ALGORITHM FOR THE PARABOLIZED
NAVIER-STOKES EQUATIONS AND COMPRESSIBLE
DUCT FLOWS

By

C. H. Cooke, Principal Investigator

Final Report
For the period April 15, 1978 - November 30, 1981

Prepared for the
National Aeronautics and Space Administration
Langley Research Center
Hampton, Virginia

Under
Research Grant NSG 1517
Douglas L. Dwyer, Technical Monitor
Subsonic-Transonic Aerodynamics Division



December 1981

DEPARTMENT OF MATHEMATICAL SCIENCES
SCHOOL OF SCIENCES AND HEALTH PROFESSIONS
OLD DOMINION UNIVERSITY
NORFOLK, VIRGINIA

A MODIFIED DODGE ALGORITHM FOR THE PARABOLIZED
NAVIER-STOKES EQUATIONS AND COMPRESSIBLE
DUCT FLOWS

By

C. H. Cooke, Principal Investigator

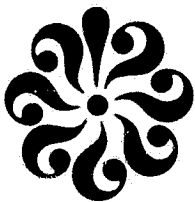
Final Report

For the period April 15, 1978 - November 30, 1981

Prepared for the
National Aeronautics and Space Administration
Langley Research Center
Hampton, Virginia 23665

Under
Research Grant NSG 1517
Douglas L. Dwyer, Technical Monitor
Subsonic-Transonic Aerodynamics Division

Submitted by the
Old Dominion University Research Foundation
P.O. Box 6369
Norfolk, Virginia 23508-0369



December 1981

A MODIFIED DODGE ALGORITHM FOR THE PARABOLIZED NAVIER-STOKES
EQUATIONS AND COMPRESSIBLE DUCT FLOWS

By

C. H. Cooke*

SUMMARY

A revised version of Dodge's split-velocity method for numerical calculation of compressible duct flow has been developed. The revision incorporates balancing of mass flow rates on each marching step in order to maintain front-to-back continuity during the calculation. The (checkerboard) zebra algorithm is applied to solution of the three-dimensional continuity equation in conservative form. A second-order A-stable linear multistep method is employed in effecting a marching solution of the parabolized momentum equations. A checkerboard iteration is used to solve the resulting implicit nonlinear systems of finite-difference equations which govern stepwise transition. Qualitative agreement with analytical predictions and experimental results has been obtained for some flows with well-known solutions.

*Professor, Department of Mathematical Sciences, Old Dominion University, Norfolk, Virginia 23508.

INTRODUCTION

It has been said that the full Navier-Stokes equations represent the ultimate mathematical model upon which to base numerical algorithms for predicting flows of practical significance. However, even with the advent of the so-called vector computers with vast virtual memory and quadrupled processing speeds, extant numerical and computational difficulties are sufficient to merit a search for simpler mathematical models and less complicated numerical methods which can still provide useful solutions to problems of interest. Thus, considerable analysis and numerical experiment has been devoted to the exploitation of parabolized marching methods for flow prediction. References 1 to 7 represent a perhaps typical but by no means exhaustive sampling of the available literature on this subject.

The parabolized marching methods are somewhat more general in application than the classical boundary-layer approach, since transverse pressure gradients are not disregarded and, in some cases, upstream influences can be transmitted through the pressure field. However, the basic assumption that streamwise viscous diffusion can be neglected restricts application to flows with a primary flow direction, limited upstream influence, and which may exhibit, at worst, crossplane recirculation. Unfortunately, in subsonic and transonic wind-tunnel flows, the elliptic upstream influence can be a significant factor in the flow dynamics; hence, interest arises in simpler mathematical models which permit this interaction. A case in point has been the development of Dodge's velocity splitting method, which allows global propagation of influence through the pressure field and which has met with

successes in both unconfined compressible and confined compressible flows (refs. 7-10). However, the method is not yet fully proven.

In this paper we shall be concerned with the application of a compressible formulation of Dodge's split velocity technique (ref. 9) to the calculation of developing flow in a square duct. The original method has been revised to effect constant mass flow rate on each transverse plane while marching down the channel. Parabolized momentum equations are employed. However, a fully elliptic pressure field is allowed by the iterative manner in which the solution of the continuity equation is coupled into the calculation procedure. Application of the presently developed computer algorithm is restricted to subsonic flow. It could readily be altered to allow transonic calculations through modification or replacement of the algorithm used to solve the conservative continuity equation.

Computational simplicity as well as numerical stability is achieved in marching the momentum equations with an A-stable (ref. 11) implicit linear multistep method, the equations of which are iteratively solved at each step by employing checkerboard successive overrelaxation. While this solution procedure may be considered expensive, the presence of quadratic as well as higher order nonlinearities in the parabolized momentum equations requires that some iteration be employed to improve accuracy. As an extra benefit, the wide-ranging stability of the resulting marching equations appears well worth the cost.

Finally, the peak efficiency of the methods developed is undoubtedly best realized on the computer system for which it has been designed, namely, the Cyber 203. For such machines, a numerical algorithm must effectively exploit the array-processing capabilities; otherwise, methods

which are not highly vectorizable misuse the available computing potential and can result in quite ordinary processing speeds. The explicit nature of the checkerboard algorithm yields a highly vectorizable method ideally suited for the array processor.

In certain parabolized marching schemes for confined flow (ref. 1), it has been the practice to decouple streamwise and transverse pressure gradients. Some argue (ref. 12) that this is necessary in order to obtain meaningful physical solutions with parabolized equations. While results are still inconclusive, computational experience gained in the current research appears to support this belief. Weak, but not total, uncoupling of the streamwise pressure gradient has appeared necessary, although this may stem from the manner in which local continuity of mass flow is enforced.

As noted by Patanker and Spalding (ref. 6), the description of a numerical procedure for solving the Navier-Stokes equations can have two aims, which are seldom possible or desirable to accomplish simultaneously. The first aim is to convey to the reader an understanding of the major principles in sufficient detail that someone with a background in the area could improvise the remainder for himself. The second aim is to present the particular equations and all approximations employed to a degree that the computational experiment could be identically reproduced. However, the second mode requires such proliferation of detail that smooth reading is impeded and understanding is inhibited. Therefore, the first aim has been chosen for the present paper, and this will be attempted in the following sections.

LIST OF SYMBOLS

C_p, C_v	specific heats
P	static pressure
ρ	density
\vec{w}	three-dimensional velocity vector
μ	viscosity
Re	Reynolds number, $\frac{\rho_o a_o D}{\mu_o}$
γ	C_p/C_v
T	temperature
$T_o, p_o, \rho_o, a_o, \mu_o$	reservoir values for temperature, pressure, density, speed of sound, and viscosity
ϕ	scalar potential
α	relaxation of parameter
D	channel half-width
M	Mach number
V_x/U	ratio of channel streamwise velocity component to entrance value

PARABOLIZED GOVERNING EQUATIONS

The nondimensional Navier-Stokes equations for compressible steady flow with which we shall be concerned are presented below.

Continuity:

$$\nabla \cdot \bar{\rho} \bar{w} = 0 \quad (1)$$

Momentum:

$$\rho(\bar{w} \cdot \nabla) \bar{w} = -\nabla P - \nabla x \frac{\mu}{Re} \nabla x \bar{w} + \nabla \frac{4}{3} \frac{\mu}{Re} \nabla \cdot \bar{w} \quad (2)$$

Energy:

$$T = T_0 - \frac{1}{2} \bar{w}^2 \quad (3)$$

Here, for flow in ducts with nonconducting walls, the usual energy equation has been replaced by the algebraic constant total temperature relation [eq. (3)]. The constitutive relations are

$$P = \frac{\gamma - 1}{\gamma} \rho T \quad (4)$$

and the viscosity approximation

$$\mu = (\gamma - 1) T. \quad (5)$$

For subsonic flow the governing equations are elliptic. However, a common approximation used to parabolize these equations (refs. 1,2) is obtained by neglecting streamwise diffusion terms in equation (2). With the exception of the entry region, the approximation is considered valid for flow in channels whose lengths are large compared to half-width (ref. 2).

Perhaps it should be remarked that when Dodge's method is applied in obtaining numerical solutions of these equations the approximation is only a partial parabolization, since the pressure field is obtained from an elliptic boundary value problem. This, of course, allows global propagation of disturbances, through the pressure field and the iteration process.

DODGE'S METHOD

Introduction

In Dodge's method, the total velocity vector \bar{w} is arbitrarily decomposed as a sum of rotational and irrotational parts:

$$\bar{w} = \nabla\phi + \bar{u} \quad (6)$$

where ϕ is a scalar potential. Pressure is hypothesized to depend solely upon the irrotational velocity according to the isentropic relationship

$$P = P_0 \left(\frac{1 - \nabla\phi^2}{2T_0} \right)^{\gamma/\gamma-1} \quad (7)$$

However, density is decomposed as the sum of a viscous contribution ρ_v and an isentropic contribution ρ^* :

$$\rho = \rho_v + \rho^* \quad (8)$$

where

$$\rho^* = \rho_0 \left(\frac{1 - \nabla\phi^2}{2T_0} \right)^{1/\gamma-1} \quad (9)$$

Substituting equations (6), (7), and (9) in equations (1) and (2) leads to the so-called split equations

$$\nabla \cdot \rho \nabla\phi = - \nabla \cdot \rho \bar{u} \quad (10)$$

and

$$\rho(\bar{w} \cdot \nabla)\bar{w} - \rho^*(\nabla\phi \cdot \nabla)\nabla\phi + \nabla x \left(\frac{\mu}{Re} \nabla x \bar{w} \right) - \nabla \left(\frac{4}{3} \frac{\mu}{Re} \nabla \cdot \bar{w} \right) = 0 \quad (11)$$

Equations (10) and (11) are to be iteratively solved: equation (10) with a 3-D relaxation method for elliptic equations, following which the parabolized version of equation (11) is marched downstream by employing a check-

erboard iteration to solve an implicit system of equations at each step. A synopsis of the iteration procedure is now presented.

Overview of Iteration Procedure

- (1) Determine a suitable initial pressure distribution P_0 by estimating a global ϕ distribution. In this investigation, pressure on the first pass is assumed to be a function of only streamwise displacement, and a mass-balancing operation establishes the initial pressure field.
- (2) Employing the current pressure field, march a parabolized version of equation (11) down the duct, simultaneously storing the right-hand side of equation (10). [See also eq. (17)].
- (3) Solve equation (10) [or eq. (17)] to obtain an updated pressure field.
- (4) Repeat the computational pass consisting of steps (2) and (3) until sufficient passes and a converged pressure field are obtained.

Dodge's Method Revised

Dodge (ref. 9) reports problems arising from adjustment of front-to-back continuity requirements with an iteration which is similar to that previously outlined. It is expected that this slow convergence stems from incomplete satisfaction of the continuity equation which could, for example, be solved after the momentum march terminates in some form such as

$$\nabla \cdot \rho_n \nabla \phi_n = - \nabla \cdot (\rho \bar{u})_{n-1} \quad (12)$$

This is in contrast to the usual parabolized marching methods, for which both mass and velocity variables are updated at each marching step.

Physically, in order to maintain continuity in a channel flow, the mass flow rate

$$\omega = \iint \rho \left(\frac{\partial \phi}{\partial x} + u \right) dydz = \iint \rho \bar{w}_{\text{normal}} dydz \quad (13)$$

must remain constant at each transverse plane. However, in Dodge's (unrevised) method this provision is only weakly incorporated through equation (10), which is solved globally upon termination of a marching pass. Thus, poor satisfaction of mass balancing during the momentum marching process is only to be expected, as numerical experimentation indicates.

Consequently, we have chosen to revise the Dodge technique in a manner which alleviates this difficulty. This was at first attempted by employing

$$\phi = \int_0^x g(\xi) d\xi + \tilde{\phi}(x, y, z) \quad (14)$$

to write equation (12) in the form

$$\nabla \cdot (\rho \nabla \tilde{\phi})_n = - \nabla \cdot (\rho \bar{u})_{n-1} - \frac{\partial}{\partial x} (\rho g)_{n-1} \quad (15)$$

The function g is determined by iterating the numerical counterpart of the parabolized equation (11) at each fixed marching step until numerical balance of mass flow rate is achieved. This is accomplished through gradual changes in streamwise velocity, pressure, and density effected by the equation

$$g^{k+1} = g^k - \alpha \left[\omega - \iint (\rho \bar{w}_{\text{normal}})^k dydz \right] + \left[\iint \rho^k dydz \right] \quad (16)$$

with α a relaxation parameter. Aside from the benefit of an instantaneous balance in mass flow rate, another merit of this device is that fewer global iterations are required in the relaxation solution of equation (15), as it is now more nearly satisfied at the outset.

However, this approach was found defective, in theory as well as in fact. The solving of equation (15) in the form indicated yields nonphysical results, as it provides a quasi-full potential transonic flow equation whose elliptic-hyperbolic transition point can differ markedly from Mach 1. This difficulty can be largely alleviated, although not totally circumvented, by replacing equation (15) with the equation

$$\nabla \cdot (\rho \nabla \phi)_n = - \nabla \cdot (\rho u)_{n-1} \quad (17)$$

whose point of transition more closely approximates the physics of the flow.

Pressure gradients in Dodge's unrevised method would be computed on pass n from the equation

$$\frac{\partial P^n}{\partial x_i} = - \left[\rho^* (\nabla \phi \cdot \nabla) \nabla \phi \right]_i^n \quad (18)$$

In the revised version, pressure gradients are allowed to develop during the mass-balancing iteration according to the equations

$$\frac{\partial P^{n,k}}{\partial x} = - \rho_{k,n}^* (g^k g_x^k + \phi_y^n \phi_{xy}^n + \phi_z^n \phi_{xz}^n) \quad (19)$$

$$\frac{\partial P^{n,k}}{\partial y} = - \rho_{k,n}^* (g^k \phi_{xy}^n + \phi_y^n \phi_{yy}^n + \phi_z^n \phi_{yz}^n) \quad (20)$$

$$\frac{\partial P^{n,k}}{\partial z} = - \rho_{k,n}^* (g^k \phi_{xz}^n + \phi_y^n \phi_{yz}^n + \phi_z^n \phi_{zz}^n) \quad (21)$$

The quantity g is determined through equation (16), and g_x by second-order backward differencing. This procedure represents a weak decoupling of the streamwise pressure gradient, since the g terms are the

dominant contributions, and since these contributions are determined from local plane-to-plane continuity considerations, somewhat independently of the output from the global continuity equation [eq. (17)] on the previous pass.

NUMERICAL ANALYSIS

The algorithm deemed most efficient for numerically solving equation (17) on the array-processing computer is the zebra algorithm of South et al. (ref. 13). This 3-D relaxation technique is in some respects similar to the hopscotch method of Gourlay (ref. 14). In equation (17) central differences are applied to all derivative terms. Variables in plane i are updated in checkerboard fashion, plane by plane in a downstream sweep, using already updated values at plane $i - 1$ and old iteration values in plane $i + 1$. Iterative repetition of downstream sweeps is used to converge the field, with a relaxation parameter employed to speed convergence.

A second-order accurate, implicit linear multistep method is used on equation (11) to march in the stepwise direction. The implicit equations are iteratively solved using a checkerboard successive overrelaxation scheme, with mass balancing built in as previously described. Streamwise derivatives are backward differenced second-order accurate, while derivatives in the (transverse) cross-plane are approximated second-order using central differences. A prediction of form

$$f_i = 2f_{i-1} - f_{i-2} \quad (22)$$

is used to initially estimate a velocity variable in plane i . The checkerboard method is then employed on the differenced counterpart of equation (11) to update variables in plane i in two cycles, with values updated on cycle 1 fed into the succeeding cycle. This two-cycle update process is iterated, employing equations (16) and (19) to (21) to alter the flow speed and pressure gradients until a balance in mass flow is achieved.

DEVELOPING FLOW IN A STRAIGHT DUCT

The revised method of Dodge has been employed to develop a finite-difference numerical model for three-dimensional viscous flows in confined regions. For boundary-layer resolution, the capability to allow individual coordinate stretching in each coordinate direction has been incorporated. The method so developed has been programmed using the SLI vector language for the Cyber 203 array processor, and appears debugged. The 32-bit half-word option of SLI has been employed in programming the zebra relaxation algorithm for solving equation (17), while 64-bit full-word arithmetic is used in programming the checkerboard marching algorithm. The program has been tested by application to the problem of computing the steady developing flow in a straight duct (see fig. 1). Boundary conditions for the problem are now given.

Boundary Conditions

Inflow: $T = T_0 - \frac{1}{2} u_1^2$
 specified velocity profiles, $\bar{W}_0 = \bar{W}(y, z)$,

$\rho_1 = R(y, z)$, $P_1 = \text{constant}$

$\phi_x(0, y, z) = g(0) = g_0$

Duct walls: velocity no slip, $\phi_n = 0$, $T = T_w$, $\rho = \rho_w$

Outflow: ρ_v extrapolated, $\phi = \phi_m$, g_m extrapolated

Artificial barriers: The computational domain is taken to be one quarter of the total duct cross section, and symmetry conditions are applied at the two resulting (nonwall) artificial barriers. Here the normal velocity component vanishes together with normal derivatives of ϕ and the other velocity variables. The variables P and T , of course, depend on ϕ and velocity at these boundaries. However, for constant total temperature, vanishing normal derivative in T , ρ is the natural boundary condition.

COMPUTATIONAL RESULTS

Introduction

An assessment of approximation error inherent in numerical solutions of parabolized flow models computed with the revised Dodge's method has been undertaken. This has been accomplished for certain flows whose solutions have been either analytically or experimentally determined and which are available for comparison with numerical results.

Two-Dimensional Channel Flow, $Re = 100$

Numerical solutions for two-dimensional, low Mach number ($M > 0.05$) flow in a straight channel have been computed, employing a uniform mesh of $17 \times 17 \times 100$ nodes. The development of the normalized centerline velocity component V_x/U characterizing the two-dimensional channel and the corresponding results of Goldstein and Kreid (ref. 15) for three-dimensional flow in a square duct are compared in figure 1. For the fully developed case Schlichting (ref. 16) gives a limiting value $V_x/U = 1.52$. The corresponding maximum value from the computational results of figure 1 is $V_x/U = 1.425$. This represents a relative error of six percent or less, depending upon how fully developed the numerically calculated flow is considered to be. One should perhaps also bear in mind that Schlichting's results come from matched asymptotic expansions, which are in themselves approximate methods. Figure 2 exhibits typical spanwise deviation from a parabolic profile characteristic of V_x at numerical full development. The maximum error is again on the order of five or six percent.

Three Dimensional Duct Flow, $Re = 100$

A $32 \times 32 \times 100$ mesh has been employed to compute low Mach number, three-dimensional flow in a square duct. Streamwise variation in centerline velocity component V_x and pressure P are shown in figures 3 and 4. A comparison between numerical calculations for V_x/U and the corresponding experimental results of Goldstein and Kraid (ref. 15) is shown in figure 5. Comparative fully developed values for V_x/U at centerline for the two cases are 1.93 and 2.10. Including grid stretching in the calculation improved the former value to 1.9725. This again represents a relative error in the vicinity of six percent.

Figures 6 to 8 show numerical performance indicators which trace the convergence history of a typical calculation. Here two kinds of outflow boundary conditions for solution of the elliptic velocity potential equation have been tested. For the calculation represented by figure 8, a Dirichlet condition was applied. Although a seemingly more rapid, nonoscillatory convergence history is observed, distortion in streamwise velocity and pressure profiles near the channel exit accompanied its application. A Neumann boundary condition appeared to eliminate these nonphysical distortions, but at the misfortune of a more sluggish, oscillatory, convergence history (see figs. 6-7). The Neumann condition was chosen for the calculations heretofore discussed.

Figures 9 and 10 show characteristics of the exit crossflow and boundary-layer profiles for the streamwise velocity component. In calculating the fully developed crossflow of figure 10, a channel length of $X_m = 12$

units with a coarse mesh having 144 downstream nodes was employed. The sink irregularity near channel centerline in figure 9 was observed to move closer to channel center as the length increased, and appeared to have coalesced with it in the calculation of figure 10. The tendency of the core flow to be directed towards channel centerline (see figs. 9 and 10) is in qualitative agreement with the theoretical predictions of Rubin (ref. 4) concerning the asymptotic behavior of duct crossflow.

CPU Time

A computer code for the revised version of Dodge's method employs the SLI-language for the Cyber 203 version of the CDC-STAR computer. With a $17 \times 17 \times 196$ mesh, measured time for program execution was found to average 2.3×10^{-4} computer resource units (CRU's) per node per model equation per pass. (This assumes only four model equations, since the energy equation was replaced with an algebraic relationship.) A pass consisted of marching the momentum equations once down the duct, iteratively solving an implicit system for velocity propagation at each streamwise station using a checkerboard scheme, and then finding the zebra solution of the three-dimensional velocity potential equation. When measuring performance in CPU seconds per node per model equation per pass, the corresponding figure becomes 4.14×10^{-4} .

SUMMARY AND CONCLUSIONS

A revised version of Dodge's velocity-split method for numerical solution of compressible confined flow has been developed. Numerical results from test calculations for low Reynolds number flow appear encouraging. In particular, qualitative but not wholly satisfactory quantitative agreement between present calculations and analytical predictions of Schlichting (ref. 16) and Rubin (ref. 4), together with experimental measurements of Goldstein and Kreid (ref. 15), has been achieved.

However, the method is by no means fully understood or exhaustively and conclusively tested. A curious feature of the present approach is the need for weak decoupling of the streamwise pressure gradient, found necessary in order to achieve a convergent numerical solution. However, Spalding (ref. 12) alleges that to obtain meaningful solutions using parabolized equations such a full decoupling is necessary. Further, Briley (ref. 1) reports successful and quantitatively accurate calculations obtained with an algorithm which incorporates this practice. Be that as it may, in this study convergence problems, first manifested by irregularities in the entrance region of the duct, were observed, but disappeared upon weakly decoupling the streamwise pressure gradient. Even so, the numerical calculations appeared overly sensitive to the treatment of the inflow, a characteristic of parabolized duct flows perhaps hinted at by Briley's suggestion of shutting off the crossflow in the first few steps of the march (ref. 1). Rubin (ref. 4) alleges that the full Navier-Stokes equations are required to properly model entry region flow. Hence, the failure to properly smear errors in this

region may have been the root problem, assuming such errors can be widely propagated, either upstream or down, in solving the elliptic velocity potential equation.

In addition to cases previously recorded, a convergent numerical solution for $Re = 1,000$ flow in a duct of length $X_m = 6$ has been achieved. However, for satisfactory calculations at high Reynolds numbers, or for longer ducts, a more powerful adaptive grid capability than is to be afforded by simple stretchings in individual coordinates appears necessary. In duct flow the driving mechanism is streamwise boundary-layer growth and concomitant flow acceleration in the core, with the induced crossflow strongest away from the walls. Hence, as the flow develops near-wall gradients decrease, or spread in extent, while core gradients grow. For high Reynolds numbers the result is that a grid system with a simple stretching mechanism set to capture entry region boundary layers is likely to become insufficient for resolving the more complex global patterns which emerge as the flow develops. Since boundary-layer thickness is thought to grow proportional to $(x/Re)^{1/2}$, it appears that the ideal grid should adaptively relax near-wall clustering in some such fashion.

The revision of Dodge's method reported herein as regards mass balancing is new, although classical in its physical origins and used previously with many other computational schemes. For flow in a straight duct it appears to be highly useful. However, the original intent of this investigation of Dodge's method was to discover its possible utility as a tool for solving the slotted wind-tunnel problem, where it was felt that the upstream influence permitted by the elliptic velocity potential equation would be highly desirable. This could well be so, were the method found workable

without resort to the mass-balancing stratagem. However, it is not felt that the present formulation with added on mass-balancing can be useful. This is because of the possibility of large pressure variations from tunnel to plenum, which would make the simultaneous balancing of mass on a plane extending over two essentially disparate channels with limited communication through the slots unfeasible, as balancing over the entire region would have to be accomplished through tuning the streamwise pressure gradient.

Possibly the most successful innovation of this investigation is the use of the checkerboard iteration as a tool for solving at each marching plane the implicit finite-differenced momentum equations. It should be noted that the checkerboard algorithm used is different from either the hopscotch method used by Rudy (ref. 17) or the recent hopscotch innovation of Greenberg (ref. 18). In both cases, iteration is not practiced in solving an implicit system; hence, the well-known inconsistency of the hopscotch method becomes significant, at least during the transient calculation. In the present case no transient exists, since the steady equations are being solved. The inconsistency of the usual hopscotch method is thus hard to bear, as it could lead to problems in solution accuracy.

REFERENCES

1. Briley, W.R.: Numerical Method for Predicting Three Dimensional Steady Viscous Flow in Ducts. J. Comput. Phys., Vol. 14, No. 1, Jan. 1974.
2. Carlson, G.A.; and Hornbeck, R.W.: A Numerical Solution for Laminar Entrance Flow in a Square Duct. J. Appl. Mech., Mar. 1973, pp. 25-30.
3. Chilukuri, R.; and Fletcher, R.H.: Numerical Solutions to the Partially Parabolized Navier-Stokes Equations for Developing Flow in a Channel. Numerical Heat Transfer, Vol. 3, 1980, pp. 169-188.
4. Rubin, S.G.; Khosla, P.K.; and Saari, S.: Laminar Flow in Rectangular Channels. Computers and Fluids, Vol. 5, 1977, pp. 151-173.
5. Hirsh, Richard S.: Numerical Solution of Supersonic Three-Dimensional Free Mixing Flows Using the Parabolic-Elliptic Navier-Stokes Equations. NASA TN D-8195, Nov. 1976.
6. Patanker, S.V.; and Spalding, D.B.: A Calculation Procedure for Heat, Mass, and Momentum Transfer in Three-Dimensional Parabolic Flows. Int. J. Heat and Mass Transfer, Vol. 15, 1972, pp. 1787-1806.
7. Cosner, R.R.: Fast Navier-Stokes Solution of Transonic Flowfield about Axisymmetric Afterbodies. AIAA-80-0193, AIAA 18th Aerospace Sciences Meeting (Pasadena, Calif.), Jan. 14-16, 1980.
8. Dodge, P.R.: A Numerical Method for 2-D and 3-D Viscous Flows. AIAA Paper No. 76-425, 9th Fluid and Plasma Dynamics Conference (San Diego, Calif.), July 14-16, 1976.
9. Dodge, P.R.: 3-D Heat Transfer Analysis Program. AFAPL-TR-77, 21-2541(7), Sept. 1977.
10. Dwyer, D.L.: Velocity Split Navier-Stokes Solution Procedure for Incompressible High Reynolds Number External Flows. NASA TN-1655, Apr. 1980.
11. Dahlquist, G.: A Special Stability Problem for Linear Multistep Methods. BIT, Vol. 3, 1963, pp. 27-43.
12. Spalding, D.B.: Numerical Computation of Steady Boundary Layers. Proceedings, Conf. on Computational Methods and Problems in Aeronautical Fluid Dynamics. Univ. of Manchester, Sept. 1974.
13. South, J.C.; Keller, J.D.; and Hafez, M.M.: Vector Processor Algorithms for Transonic Flow Calculations. Proc. of AIAA Fourth Computational Fluid Dynamics Conference (Williamsburg, Va.), July 23-24, 1979.

14. Gourlay, A.R.: Hopscotch: A Fast Second-Order Partial Derivative Equation Solver. J. Inst. Math. Appl., 1970, Vol. 6, pp. 375-390.
15. Goldstein, R.J.; and Kreid, D.K.: Measurement of Laminar Flow Development in a Square Duct Using a Laser Doppler Flow Meter. J. Appl. Mech., Dec. 1967, pp. 813-818.
16. Schlichting, Herman: Boundary Layer Theory. McGraw-Hill, 1960.
17. Rudy, David H.; Morris, Dana K.; Rubin, Stanley; and Cooke, C.H.: An Investigation of Several Numerical Procedures for Time Asymptotic Compressible Navier-Stokes Equations. NASA SP-347, 1975.
18. Greenberg, J.B.: Some Semi-Implicit Hopscotch Type Methods for the Time Dependent Compressible Navier-Stokes Equations. AIAA Paper 81-1022, AIAA 5th Computational Fluid Dynamics Conference (Palo Alto, Calif.), June 22-23, 1981.

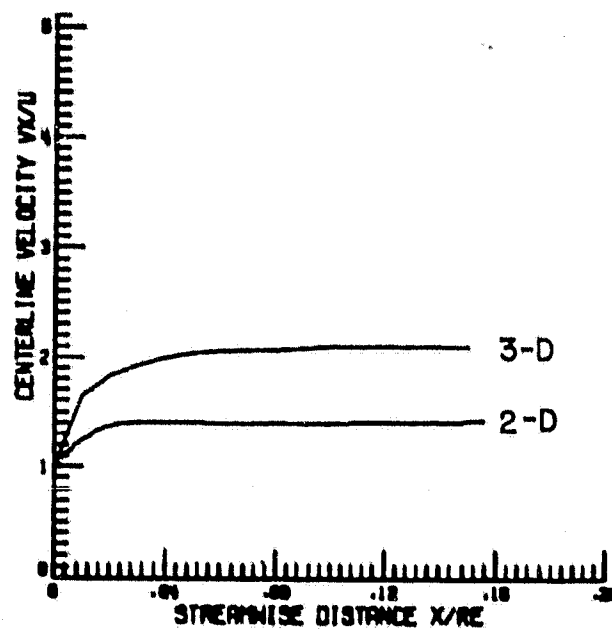


Figure 1. Comparison of normalized centerline velocity development for two and three-dimensional channel flow.

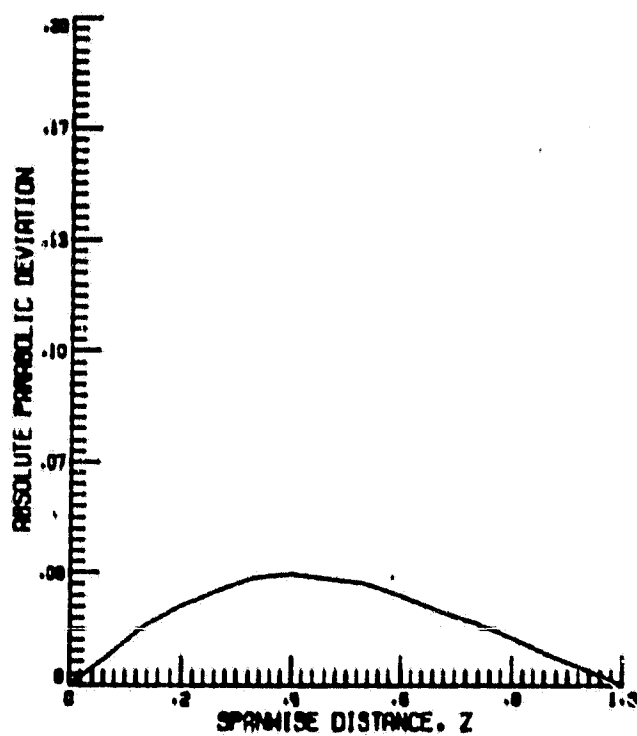


Figure 2. Deviation from a parabolic profile of the streamwise velocity component at outflow - two-dimensional flow.

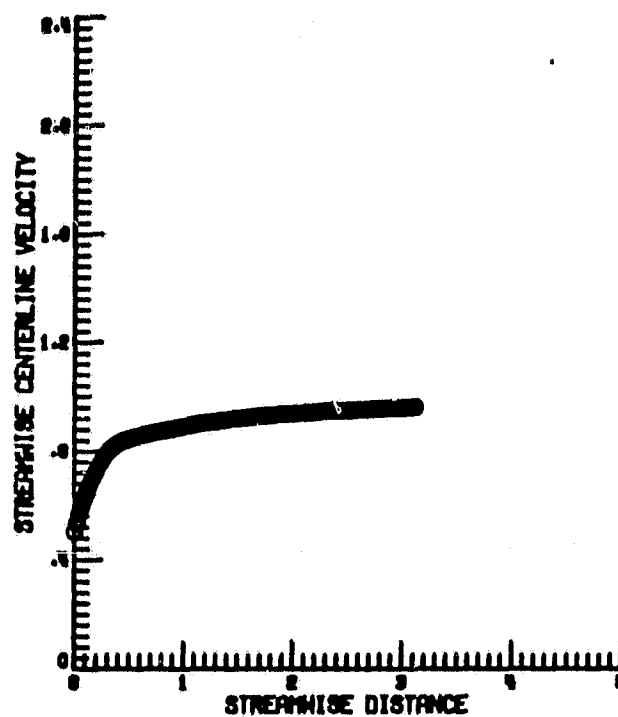


Figure 3. Flow development for streamwise velocity component - three-dimensional duct flow.

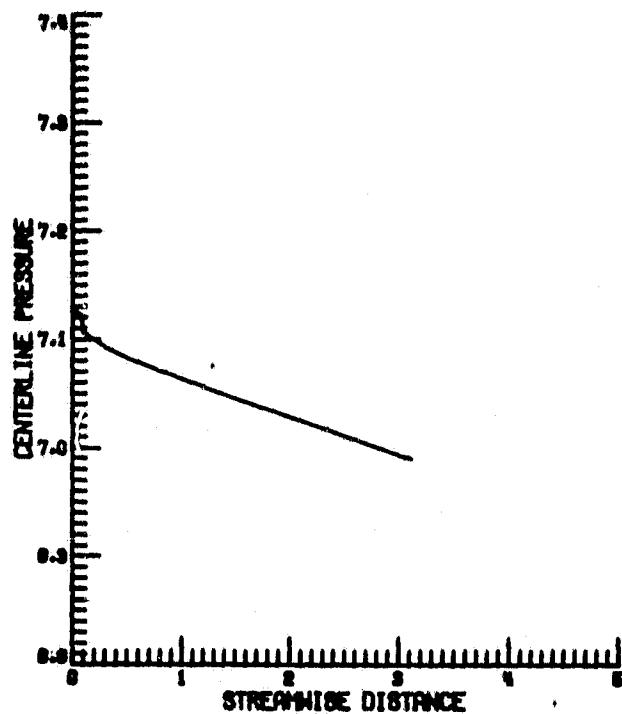


Figure 4. Streamwise development for centerline pressure - three-dimensional duct flow.

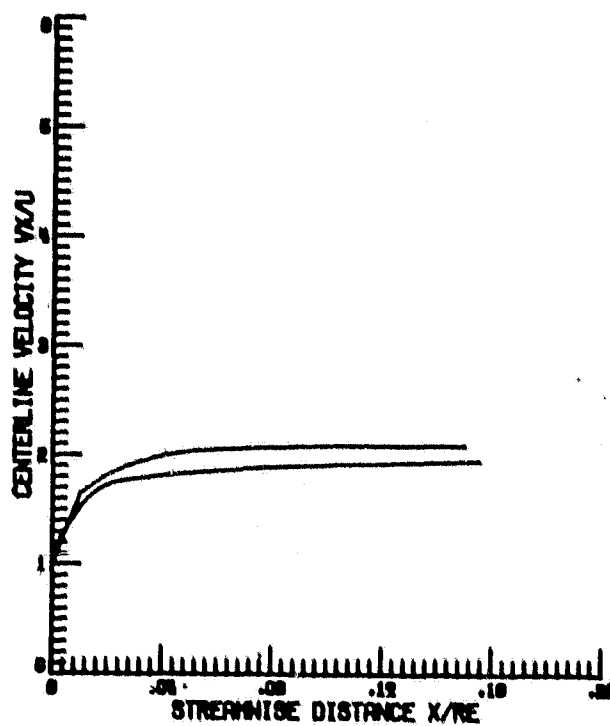


Figure 5. Experimental versus computed development for streamwise velocity component - three-dimensional duct flow.

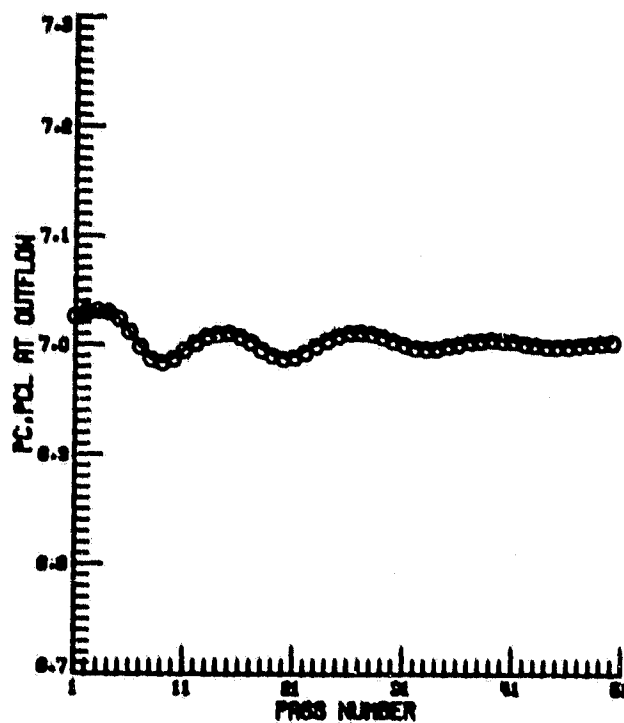


Figure 6. Iteration history, corner and centerline pressure at the outflow - Neumann condition.

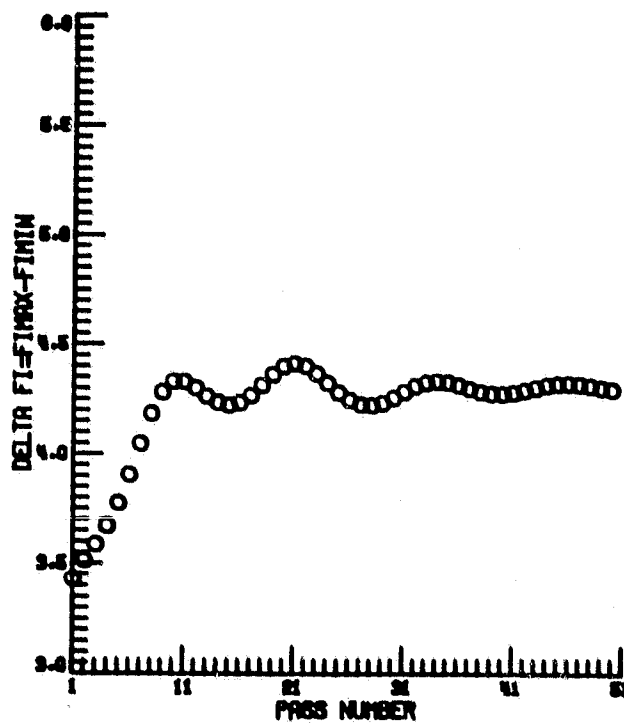


Figure 7. Iteration history, streamwise increment in velocity potential - Neumann condition at outflow.

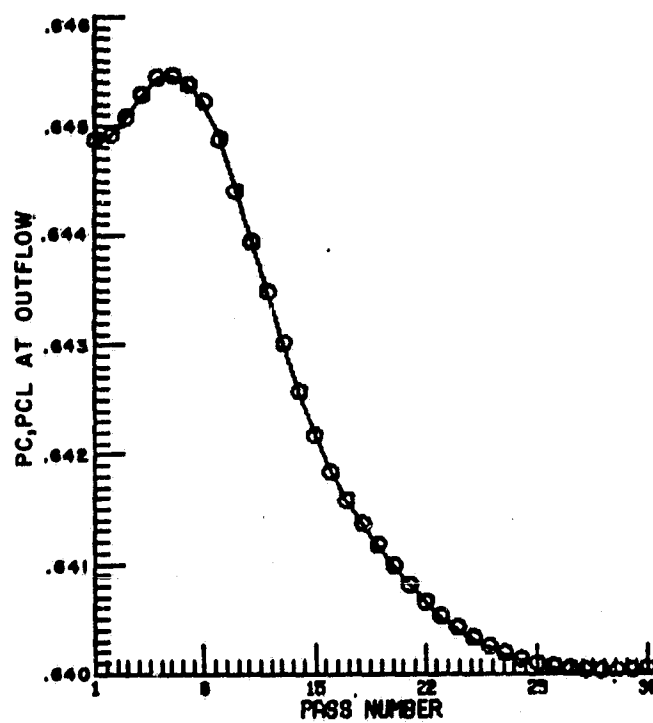


Figure 8. Iteration history, corner and centerline pressure at outflow - Dirichlet condition on velocity potential.

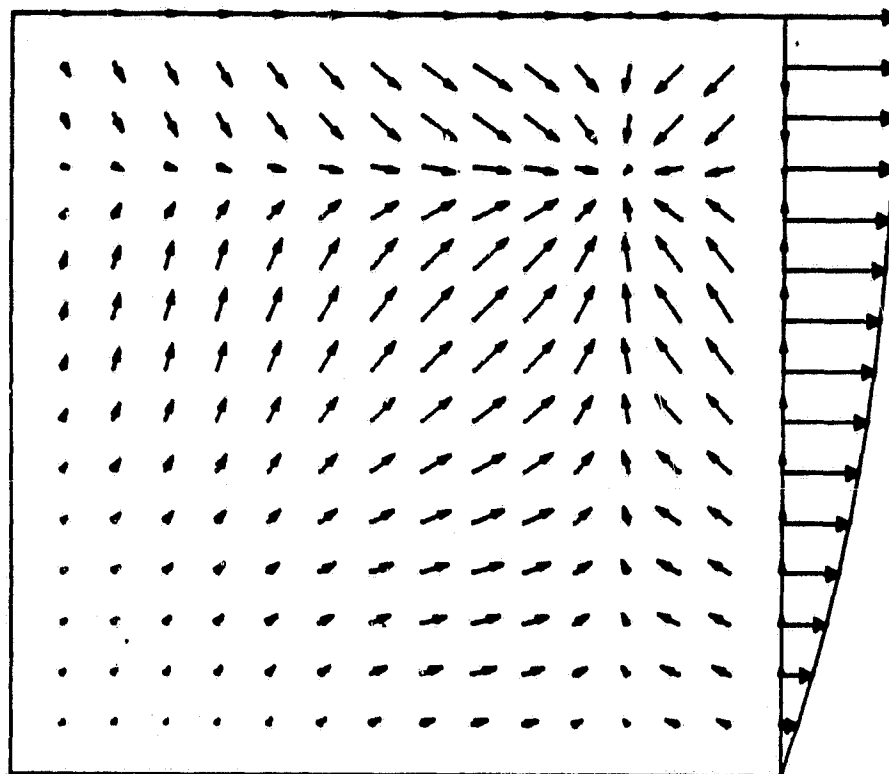


Figure 9. Crossflow and boundary-layer profile for streamwise velocity component at channel exit, $Re = 100$, $X_m \approx 3.0$.

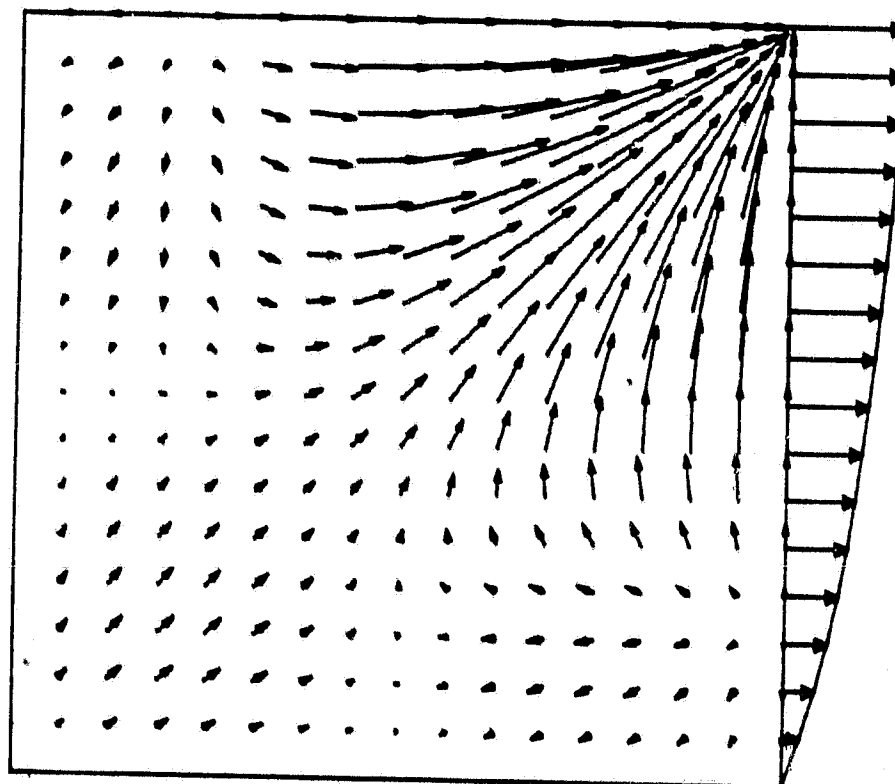


Figure 10. Fully developed exit flow, $Re = 100$, $X_m = 12.0$.